ELSEVIER

Thermochimica Acta 280/281 (1996) 417–447

thermochimica acta

The transition points in the liquid state and their molecular modeling[1]

B. Hlaváček [a,*], E. Černošková [b], L. Prokůpek [a], M. Večeřa [a]

[a] *University of Pardubice, Dept. of Polymers, Pardubice, Czech Republic*
[b] *Joint Lab. of Solid State Chemistry of Czech Academy of Science and University of Pardubice, Pardubice, Czech Republic*

Abstract

A unified approach leading to the understanding of the liquid state has been developed. The liquid state is characterized by the onset of non-linear anharmonic vibrations at T_g, and is connected with the first appearance of vacancies.

The second boundary temperature for the liquid state "T_c" is understood as the temperature at which (as a result of an overabundance of holes) the continuous phase can no longer exist and the "foamy" structure of the liquid disintegrates into clusters. The p_c value is connected with the cohesive energy density and also depends on Pitzer's acentric factor which itself can characterize the type of bonding (local versus dispersed) of the molecule within the liquid phase. The critical volume of individual compounds seems to be mainly connected with the high-frequency electronic vibrations of individual atoms and their polarizabilities. The critical volume is usually about 50–55 times larger than the summation of individual electronic polarizabilities of the atoms from which the characteristic substance is made.

Keywords: Atomic polarizabilities and their relation to critical volumes; Cohesive energy density; Critical parameters T_c, V_c, p_c; T_c transitions; T_g transition; Theory of holes and T_g

List of symbols

A	subscript: for characterization of system A
A	amplitude
A_1	amplitude

* Corresponding author.

[1] Dedicated to Professor Hiroshi Suga..

SSDI 0040-6031(95)02783-1

A_2	amplitude
A^*	constant for the expanded Hamiltonian
B	subscript: for characterization of system B
B^*	constant for the expanded Hamiltonian
C	constant from Eq. (6) related to the configurational entropy
C.E.D. $= \delta^2$	cohesive energy density
D_r	relative deformation ξ/r_0
E_n^0	standard nth energy level
E_n	shifted nth energy level
$F_1(T_{rB};\omega)$	function of the acentric factor ω and the relative temperature at the boiling point
$F_2(\omega) = \dfrac{0.501\omega + 0.395}{T_{rB}}$	where T_{rB} is expressed through one of Eqs. (66)
$F_3(\omega;\log p_c)$	function of acentric factor ω and log p_c; the implicit dependence on p_c is a result of substitution of Eq. (68) into Eq. (56), (64)
H_0	classical Hamiltonian (Eq. (23))
$H = H_0 + \vartheta$	expanded form of the Hamiltonian (Eq. (25))
$K^* = f/r_0$	model of the material in compression
K_1, K_2, K_3	constants of Eqs. (2)–(4)
L	latent heat of evaporation
N_{AV}	Avogadro's number
P_{exp}	experimentally measured molecular electronic polarizibility
P_A	molecular electronic polarizibility obtained from the summation of the polarizibilities of individual atoms
R	universal gas constant
S	entropy
S_c	configurational part of the entropy
S_{th}	thermal part of the entropy
T	temperature in K
T_g	glass transition temperature
$T_g(T)$	glass transition temperature for indefinitely small speeds of temperature change
$T_g(\infty)$	Vogel's temperature for indefinitely small speeds of temperature change $T_g(\infty) + 52 = T_g(T)$
T_m	melting point temperature
T_{rB}	relative temperature at boiling point
T_c	critical temperature
U	energy of cohesive forces
U_0	bottom level of cohesive energy
V_c	critical volume
a	cohesive energy × volume; $a = \dfrac{27}{64}\dfrac{R^2 T_c^2}{p_c}$
a_A	cohesive energy × volume for system A

a_B	cohesive energy × volume for system B
a_{AB}	mutual interaction term $a_{AB} = (a_A a_B)^{1/2}$ of system A and B
$a(T)$	Peng–Robinson cohesive energy × volume constant
a_1	upper constant in the WLF equation (usually $a_1 = 17.4$)
a_T	relative shift in the relaxation time as a result of temperature change from T_g to $T > T_g$
$b = \frac{1}{8}\frac{RT_c}{p_c}$	constant of volume in the van der Waals equation of state
$b(T)$	second Peng–Robinson constant $b = 0.0778\frac{RT_c}{p_c}$
b_A	constant of particles volume in pure system A
b_B	constant of particles volume in pure system B
c	constant reflecting the softening of particle vibrations at high amplitudes (Eq. (35))
c_p	specific heat at constant pressure
Δc_p	change in specific heat at constant pressure during a second-order transition
d	subscript: abbreviation for the dispersion forces
f	proportionality constant of harmonic force [energy/length^2]
f_g	fraction of free volume at T_g (usually $f_g = 0.025$)
g	function of potential valley distortion [energy per volume] in a liquid state
g'	function of potential valley distortion in a solid state $g' \ll g$
h	Planck's constant
i	subscript
k	Boltzman's constant
m	mass of a particle
n	index
n_0, n_1, n_2	number of particles connected with the baseline lowest energy level, number of particles connected with a higher energy level (n_1), etc.
n_0	number of holes
n_x	number of polymer molecules each occupying "x" lattice sites
p	subscript for the polar forces contribution
p_c	critical pressure
p_s	saturation pressure at $T_r = 0.7$
r_0	distance separating two bottoms of neighboring potential valleys
$v_f(T)$	free volume
v_g	free volume at $T = T_g$
x_A, x_B	molar fractions of substance A and B
x	number of occupied sides per polymer molecule

Greek letters

α	coefficient of thermal expansion
$\tilde{\alpha}$	temperature- and acentric-factor-dependent part of the Peng–Robinson function $a(T)$
α_f	coefficient of thermal expansion for a liquid
α_g	coefficient of thermal expansion for a glass
α_1	coefficient of thermal expansion associated with a low level of perturbation function
α_2	coefficient of thermal expansion associated with a high level of perturbation function
δ	solubility parameter based on the definition either in Eq. (44) or Eq. (44). Eq. (48) is valid only for the case of special interaction expressed through Eq. (48)
δ_d^2	contribution to C.E.D due to the dispersive forces
δ_p^2	contribution to C.E.D due to the polar forces
δ_h^2	contribution to C.E.D due to the hydrogen bond forces
δ_{PR}	solubility parameter defined based on the constants of the Peng–Robinson equation $\delta_{PR} = \dfrac{a^{1/2}(T)}{b(T)}$
δ_{BPR}	solubility parameter defined based on the Peng–Robinson equation at the boiling point
$\delta_{COR,B}$	corrected parameter δ_{BPR} (general expression defined through Eq. (63))
$\delta_{COR,B,1}$	corrected parameter δ_{BPR} based on Eqs. (64) and (65)
$\delta_{COR,B,2}$	second correction for the parameter δ_{BPR} based on the expression of T_{rB} from the empirical equations of (66)
$\delta_{COR,B,3}$	third correction for the parameter δ_{BPR} based on the universal expression for T_{rB} (Eq. (69))
κ	function of ω in the Peng–Robinson equation
ρ_0	density of liquid at $T=0$
ρ_c	density of liquid at $T=T_c$
ξ	coordinate signifying the deviation of a particle from the bottom of potential valley, $\xi = r - r_0$
$\bar{\xi}$	average value of coordinate
$\bar{\xi}_1$	average value of the oscillations of the individual particle below T_g
$\bar{\xi}_2$	average value of the oscillations of the individual particle above T_g
υ	frequency of the particle oscillations below T_g (Eq. (20))
Ω	frequency $\Omega = \omega_1 - \omega_2$ for the special case of an anharmonic oscillator $\omega_1 = \omega$ and $\omega_2 = 2\omega$
ϑ	perturbation part of the Hamiltonian
ϑ_{nm}	change in the "n" energy level

ψ_n^0 characteristic wave function
ψ_n^{0*} complex adjoin wave function

1. Introduction

For the rheologist, a Newtonian liquid is characterized as a liquid obeying Newtonian law which states the proportionality between the stress component and the velocity gradient [1]. Any motion of such a liquid will be characterized by dissipation of energy into heat. No elastic energy can be stored (with the exception of bulk deformation) in such a fluid. Low molecular weight substances usually fulfil the Newtonian law in the area of temperatures above their melting point or above their glass transition temperatures. The fluidity of low molecular weight substances is usually roughly proportional to their free volume [2–5]. The viscosity decreases as the free volume grows and the temperature rises. This is in contrast to gases, in which the viscosity rises with temperature increase, as a result of the increase in the momentum energy transfer between the moving layers of the continua [5, 6]. On the microlevel, above T_g or T_m, the liquid contains a certain amount of rapidly moving vacancies (Fig. 1). The structure is characterized by potential valleys at the bottom of which the particles exercise oscillatory motion. In the liquid state, the shape of the potential valley allows the particles to move without any change at a constant potential energy level (Figs. 2, 3) [7, 8]. It is usually assumed that the number of vacancies is small (slightly more than 2.5% by volume above T_g and a little more than 7% above T_m) [9]. The onset of first vacancies is well described in polymer rheology [10, 11], where the fact that about 2.5% of the vacancies exist at T_g gives a basis to the famous Williams–Landel–Ferry (WLF) equation [11] which allows the superposition of time–temperature experiments for a vast number of liquids. It is interesting that the idea of how many vacancies exist at the boiling point of a liquid or under critical conditions has never been put forward nor provoked any special interest. We will follow this idea further and try, with the help of thermodynamic theories, to elucidate the critical state.

The most important classical feature of equilibrium thermodynamics is that this science always studies the system at rest, not using the time derivative at all. On many occasions, scientific study has derived support from the equation of state theories [12, 13].

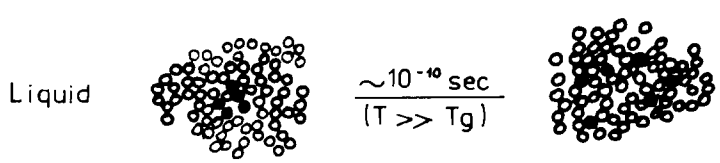

Fig. 1. A picture of the liquid state according to Graesley [7]. The black points represent the vacancies rapidly diffusing through the body of particles.

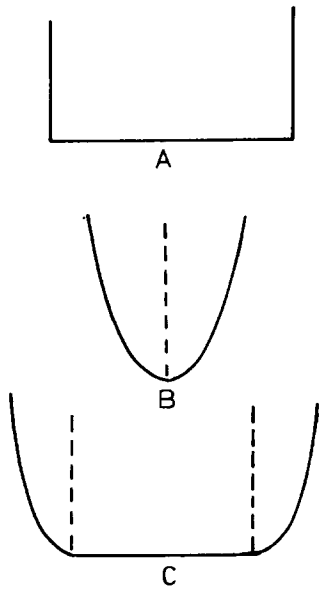

Fig. 2. Potential energy of molecule in a cell (according to Hirschfelder et al. [8]): A is the simplest version of the liquid; B is the solid; C is the potential for a molecule in the liquid which leads to the correct heat capacity.

In our study, we have emphasized the two points between which the liquid state can exist, i.e. T_g and T_c. We will try to show that all liquids have a similar structure and show a similar behavior in the vicinity of these two points. Regarding liquid polymers, it is known, of course that polymers can never form a gas phase [10, 11] as a result of their

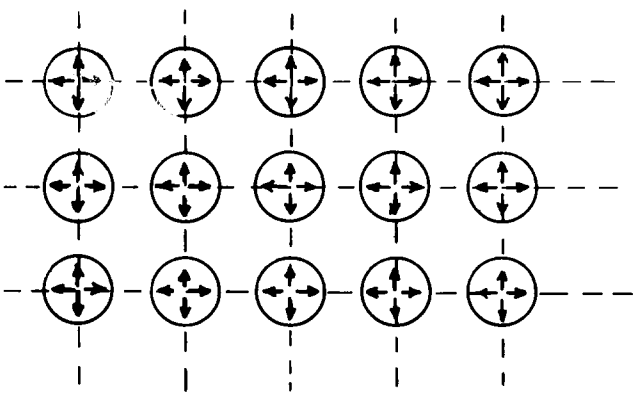

Fig. 3a. Schematic representation of solids. The individual particles are vibrating around their equilibrium position. Any displacement of the particle from the bottoms of the potential valleys is associated with a change in potential energy level of the particle.

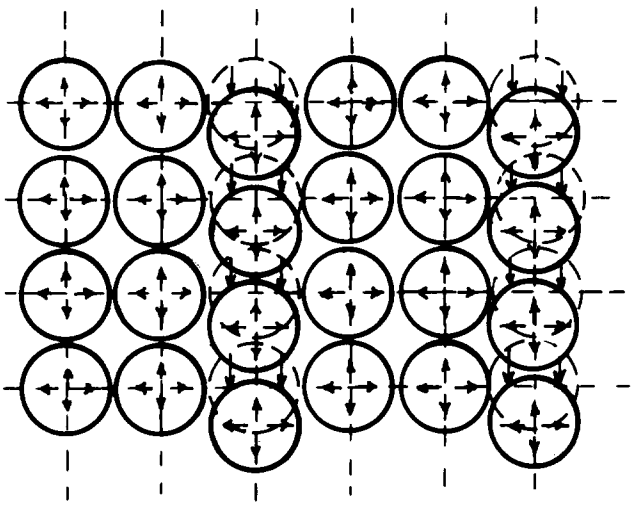

Fig. 3b. Schematic representation of liquids. The individual particles are vibrating around their equilibrium positions. However, a coordinated "shift" or "slide" of several particles does not have to be connected with any change in the potential energy level. The "slide" proceeds over the bottoms of "pan-like" potential valleys.

entanglements. Nor can polymers reach the critical state because their macromolecules will thermally disintegrate before they reach critical conditions. However, some parameters such as p_c (the critical pressure) can have some meaning even for polymers. The critical pressure can provide an important insight into the problem of solubility and cohesive interaction energy, and is quite unimportant if the p_c value comes from the monomer value (where p_c can be either measured or calculated [14, 15]) or from a hypothetical p_c for the polymeric subsegment (where the p_c can only be calculated) from the fragments of monomeric unit, etc.

2. The limiting points of a liquid state

The liquid state can generally be characterized by two extreme boundary points. One point is T_g or T_m where the liquid state comes into existence. The second boundary forms the T_c point. Here we deliberately avoid such phenomena as the long-term creep of solids or phenomena observed above T_c under extreme high pressure conditions. With the exception of polymers, which as a result of their entanglements, cannot form a gas phase, substances in the liquid phase usually find themselves in equilibrium with a gas phase [12, 13]. See also Fig. 4, below.

The liquid forms a foamy structure, in which the number of holes or vacancies can vary widely from 2.5% at T_g to about 400% at T_c.

At T_c, the liquid phase is so disintegrated by the presence of holes that the individual molecules can no longer be put together in such a way as to form a continuous phase.

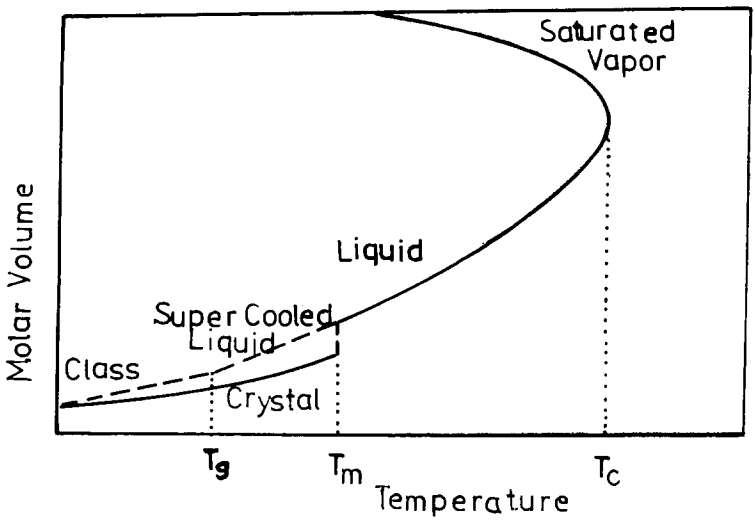

Fig. 4. The molar volume of a liquid as a function of temperature.

We will now look more closely at the descriptions of the liquid structure at T_g or T_c, provided the pressure does not exceed the usual level of critical pressures of organic compounds ($p_c < 70$ atm) or water (217 atm). Under these pressures, the vacancies (or holes) in liquids can be considered to be incompressible [16].

We will then investigate the liquids from the point of view of cohesive energy density, solubility, etc., within the limit of the (T_g; T_c) interval.

3. The T_g transition

Numerous literature references exist [10, 11, 17–29] which deal with the topics of the T_g transition. This traditional area, which the tremendous success of the WLF equation [30, 31] has made the most identified and precisely described area in polymer science, is the major emphasis of this study and is considered from new points of view.

Because both constants, 17.4 and 52 K, in the WLF equation can be pictured as the sides of a triangle at T_g, as well as the fact that the WLF equation provides us with a visual picture of the T_g transition, with the notion of 40 particles per vacancy (Fig. 6), this presents a rare example in science in which mathematical numbers can be substantiated and envisaged in the form of a physical model: $f_g = 0.025 = 1/40$; $17.4 = 40/2.303$, where the factor 2.303 is connected to the inversion of $\log x = 2.303 \ln x$, used on the left-side of Eq. (1)

$$T_g(T) - T_{g(\infty)} = 52\,\mathrm{K}$$

$$\alpha_f = 4.8 \times 10^{-4}\,\mathrm{K}^{-1}$$

$$\text{WLF} \quad \log a_T = \frac{17.4(T - T_g)}{52 + T - T_g} \tag{1}$$

The vast majority of amorphous polymers can be successfully treated for the time–temperature superposition using this equation. The value of $a_T = \tau_T/\tau_{T_g}$ in Eq. (1) represents the relative shift in the relaxation times as the result of temperature increase from T_g to T. The T_g transition itself, as a second-order transition, shows a stepwise change in the coefficient of thermal expansion α and c_p value. (As a second-order transition we consider an area in which the first derivative of a thermodynamic quantity, V, H, etc., shows a stepwise change. So the word "derivative" is used to indicate "second-order". For the first-order transition, the quantity, V, H, etc., itself shows a stepwise change at such a point.)

In a series of papers Simha and Boyer [32–34,48] have concluded that

$$\Delta\alpha T_g = K_1 = 0.113 \tag{2}$$

$$\alpha_f T_g = K_2 = 0.164 \tag{3}$$

$$\Delta c_p T_g = K_3 = 25\,\text{cal g}^{-1} \tag{4}$$

Sharma et al. [35] then confirmed the validity of Eq. (2) but only as a very crude approximation, with substantial dispersion of experimental data values. The validity of Eq. (2) will mean that $\Delta\alpha$ has to be changed as T_g increases and, therefore, either the constant 17.4 or 52 in Eq. (1) must also be varied. Thus, in Eq. (2) Simha and Boyer [32–34] have put a restriction on the WLF equation. This has never been mentioned before. This seems to be the opposite of the work of Adam and Gibbs [36] who assume the constancy of the triangle in (Fig. 5) for their calculations of c_p. The successful work

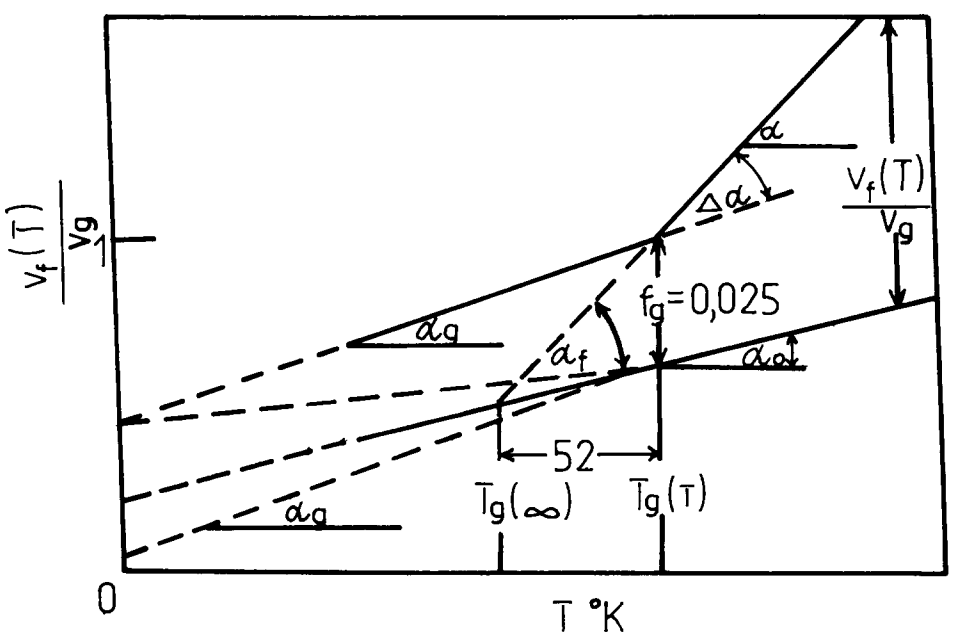

Fig. 5. Schematic variation of total specific volume, occupied volume and free volume (after Ferry [11] and Kovacs [23, 24]).

of Havlíček and co-workers [21, 22] in the prediction of Δc_p, also follows this [35] direction.

For the T_g temperature, it is valid that the energy of thermal vibration of individual atoms or vibrating units must reach a certain value in relation to the cohesive energy density [37]. The cohesive energy densities of a few polymers are available in the literature [38, 39]. A similar approach relating T_g to the vibrational energy per segment was developed by Becker [40, 41] and Kreibich and Batzer [42]. The connection with the vibrational energy at the T_g transition was also recently introduced with a new approach by Hlaváček et al. [43]. Before describing their approach more closely, we will outline the traditional way of dealing with the T_g transition, in the sense of Gibbs [19] and Flory [29]. Di Marzio [45] extended Flory's idea about the miscibility of polymers with limited flexibility by introducing the number of holes created into the partition function describing the system. The definition of α introduced by Di Marzio was based on the number of holes $\bar{n}_0$ [36]

$$\alpha = \frac{\frac{\partial(\bar{n}_0)}{\partial T}}{n_0 + x\mathrm{n}_x} \tag{5}$$

where n_x is the number of polymer molecules each occupying "x" lattice sites, and c_p is related to the free volume at T_g, i.e. the WLF constant $a_1 = 17.4$ [45]

$$a_1 = 2.303\frac{C}{\Delta c_p T_g\left(\frac{T_g}{T_{g(\infty)}}\right)} \tag{6}$$

where the constant C is related to the configurational entropy and Gibbs energy [45]. The Di Marzio–Gibbs–Adams approach has been broadly discussed by Ritchie [18]

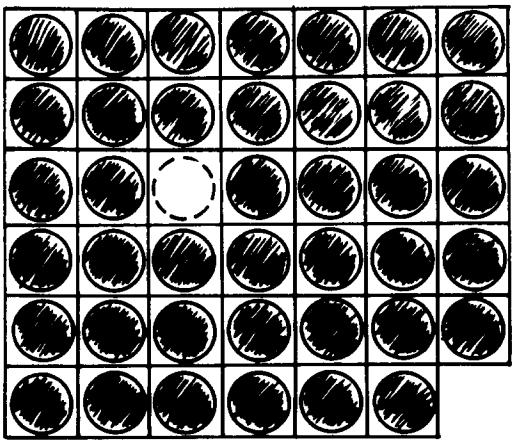

Fig. 6. Alternative model for a liquid phase at T_g (1 vacancy: 40 particles).

and also by Meissner and Zilvar [46]. It is sometimes strongly argued [18, 46] that the T_g point does not even represent the equilibrium transition because, the individual particles being limited in their motion (according to Kauzman [47] the time for one jump per particle at T_g is several hours), cannot reach the lower level of energies under T_g.

Thus, under T_g the system is characterized by a nonequilibrium partition function. The disadvantage of the Di Marzio approach lies with the flexibility function, which he introduced. This function is supposed to undergo a sudden change at T_g, thus causing a rise in the Δc_p and $\Delta\alpha$ functions. The Δc_p undergoes changes similar to the Dirac Δ function at T_m; however, above T_m the Δc_p for many substances returns to its value under T_m and thus does not change drastically, despite the fact that the free volume undergoes a stepwise change and about 7–10% vacancies are created [9]. In reality, according to experimental data, the Δc_p at T_g changes more than Δc_p changes above T_m, where the chains must undergo considerable far-reaching changes in their flexibility. (See data for polyethylene presented by Brydson [39, 49] or for inorganic substances presented by Frenkel [9].) The limitation of the Di Marzio approach regarding the T_g, T_m-sensitive differentiation, the flexibility function problem, and also the limitations regarding inorganic glass treatment, has led us to consider an alternative dynamic treatment, which can be regarded as being complementary to the previous theories, which are not rejected.

4. The dynamical view of the T_g transition

Solid state physics [9, 29, 50–52] suggests a different origin of the thermal expansion coefficient from that of polymer science. The definition according to Eq. (5) is essentially unknown in solid state physics. Solid state physics assumes that the "skew" character of the potential valley in which the individual particles undergo thermal motion plays a crucial role in the definition of α. The change in the shape of the potential valley from purely parabolic to skew can serve as the explanation of the T_g transition.

5. The coefficient of thermal expansion

According to Einstein [53] and Debye [54], the heat of solids is connected with the vibration of particles around their equilibrium positions. Every particle of mass m which sits in a potential hole U is characterized by its parabolic shape

$$U = U_0 + \frac{1}{2} f \xi^2 \tag{7}$$

and undergoes harmonic oscillations under the influence of the force

$$F = -\frac{dU}{d\xi} = -f\xi \tag{8}$$

and exhibits harmonic oscillations which are characterized by the frequency

$$\upsilon = \frac{1}{2\pi}\sqrt{\frac{f}{m}} \tag{9}$$

where U_0 is the basic level of internal energy U; $\xi = r - r_0$ is the deviation from the equilibrium position where r_0 is defined as the distance separating two bottoms of neighboring potential valleys. And $f = \mathrm{d}^2U/\mathrm{d}\xi^2 > 0$ is the coefficient of the quasi-elastic force, connected to the bulk modulus K^* [9], where $K^* = f/r_0$. According to Müller [52], substances like Invar or carbon are distinguished through harmonic oscillations according to Eqs. (7) and (8), and the character of potential holes which is defined by Eq. (7) does not change with an increase in temperature. The fact that in a liquid the character of a potential hole is not a paraboloid but "pan-like" has already been mentioned by Hirschfelder et al. [8] and has recently been studied in detail by Luck [55].

According to Müller [52] and Frenkel [9] every compound for its thermal expansion needs to vary the shape of the potential valleys in which the individual particles are located. The change in the shape of the potential valleys is the only way to achieve thermal expansion of substances with temperature. Such change, however, will influence the strict character of the harmonic motion of individual particles. For our purposes of T_g consideration, it seems sufficient to add just one perturbation term to Eq. (7). This allows us to illustrate the point

$$U = U_0 + \frac{1}{2}f\xi^2 - \frac{1}{3}g\xi^3 \tag{10}$$

We consider the one-dimensional case only which is assumed for substances which distinguish themselves by a very small coefficient of thermal expansion (the function $g \to 0$). For the choice of thermal energy $U_0 = 0$, the energy U has to be that for substances which distinguish themselves by a very small coefficient of thermal expansion equal to the energy of thermal motion kT, where k is Boltzmann's constant. We get

$$U = \frac{1}{2}kT = \frac{1}{2}f\bar{\xi}^2 \tag{11}$$

where $\bar{\xi}^2$ is the average quadratic deviation from the bottom of the potential valley. The average value of the distance between the particles remains constant and equal to r_0 since the mean value of $\bar{\xi}$ vanishes. This gives us

$$\bar{\xi}^2 = \frac{kT}{f} \tag{12}$$

where k is Boltzmann's constant.

Let us now consider the case of an anharmonic force F acting in a non-ideal case when the particle sits in a potential valley given by Eq. (10)

$$-\frac{\mathrm{d}U}{\mathrm{d}\xi} = F = -f\xi + g\xi^2 \tag{13}$$

Equating its mean value to zero we get

$$F_{AV} = 0 = -f\bar{\xi} + g\bar{\xi}^2 \tag{14}$$

Eq. (14) gives us the relation connecting the average deviation $\bar{\xi}$ with the shape of the potential valley for real substances. We get

$$\bar{\xi} = \frac{g}{f}\bar{\xi}^2 \neq 0 \tag{15}$$

For the harmonic oscillations, $\bar{\xi}$ would be zero. We can see that as a result of the anharmonic character of the thermal motion, the average position of particles $\bar{\xi}$ has been shifted. Providing that the particles are separated by distance r_0 and the change in the character of motion for the temperature change dT has been characterized by an increase in g from $g' \to 0$ to g, then for the relative displacement D_r and coefficient of thermal expansion α, we get

$$D_r = \frac{\bar{\xi}}{r_0} \tag{16}$$

Substituting from Eq. (12) into Eqs. (15) and (16) we get

$$\alpha_1 = \frac{1}{r_0}\frac{d\bar{\xi}_1}{dT} = \frac{1}{r_0}\frac{g'}{f^2}k \tag{17}$$

$$\alpha_2 = \frac{1}{r_0}\frac{d\bar{\xi}_2}{dT} = \frac{1}{r_0}\frac{g}{f^2}k \tag{18}$$

where α_1, α_2 are the coefficients of thermal expansion for two different levels of the perturbation function g', g in the solid–liquid transition

$$\Delta\alpha = \frac{1}{r_0}\frac{d\Delta\bar{\xi}}{dT} = \frac{1}{r_0}\frac{g-g'}{f^2}k \quad \text{where} \quad \Delta\alpha = \alpha_1 - \alpha_2 \tag{19}$$

From Eqs. (14)–(19), we can see that the coefficient of thermal expansion can be associated with the anharmonic character of the thermal vibrations. Its sudden change at T_g is thus also associated with different characteristics of thermal motion of the particles. At that transition not only does the rigidity of the substance play a role in the change in α, which is expressed by the presence of the function "f", but also the perturbation function g–g' regarding the shape of the potential valley makes the sudden change in α possible. We can now associate the change in α in Eq. (19) with the change in α at T_g. We arrive at a new understanding of the T_g transition, which associates the T_g transition with the onset of a new form of vibration, which is pertinent to every particle of the system. As shown by Kittel [51], the consideration of a higher term in the perturbation term function does not change the final results in the α term.

6. The change in the characteristics of the vibrational frequency

From Eqs. (14)–(19) it can be seen that the T_g transition can be envisaged as a sudden variation in the function g. If we take the substance as an ensemble of vibrating harmonic oscillators which move with characteristic frequency under T_g

$$\upsilon = \frac{1}{2\pi}\sqrt{\frac{f}{m}} \tag{20}$$

where m is the mass of individual particles, then above T_g (where we assume that the anharmonic character of the motion takes place), a new term appears in the solution for ξ [50]. For $\omega = 2\pi\upsilon$, the anharmonic oscillator, we get, according to Kittel et al.

$$\xi = \tilde{A}\left(\cos\omega t - \frac{1}{6}\frac{g}{f}\cos 2\omega t\right) \tag{21}$$

The solution for the anharmonic oscillator is characterized by two different frequencies. The influence of the second term depends on the ratio of g/f. The fact that such an oscillator can absorb the energy at two frequencies can be understood as the increase in the number of oscillators characterizing the system. The higher number of oscillators can loosely explain the Δc_p changes at T_g.

Choosing $A_1 = \tilde{A}$ and $A_2 = -1/6g/f\tilde{A}$ for the final amplitude of the "wobbling" motion, we can get

$$\tilde{A} = \{A_1^2 + A_2^2 + 2A_1A_2\cos\Omega t\}^{1/2} \tag{22}$$

where

$$\Omega = \omega_1 - \omega_2$$

For the special case of $A_1 = A_2$ the phenomena can be nicely visualized (Fig. 7). The onset of anharmonic motion above T_g is connected with an increase in the average

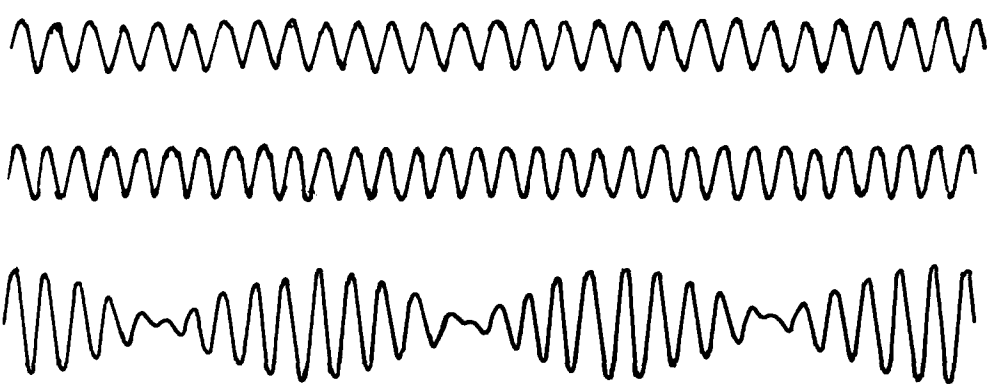

Fig. 7. A schematic view of the motion of an harmonic oscillator characterized by angular frequency ω_1 (top), angular frequency ω_2 (middle), and the anharmonic oscillator characterized by two frequencies, ω_1, ω_2, and Eq. (22) for the case $A_1 = A_2$ (bottom).

amplitude of vibrational motion as well as with the onset of motion which is characterized with a different frequency. This change, which results in a sort of wobbling motion, affects every particle of the system. This would also affect the sharp change in the fluidity of the system above T_g, which the "static" notion of the imperfections or defects in the lattice structure (1 hole per 40 particles) can hardly explain. The perturbation term g must always compensate the shape of the bottom of the potential valleys in such a way that for a very small displacement of particles the term, $dU/d\xi = 0$, which is a characteristic of a liquid state. We hope this approach provides a complementary addition to the previously mentioned theories. [16–28, 30, 32–37, 40–44]. The problem can now be demonstrated by the entropy function.

Instead of having the problem defined only by S_c in the sense of the Di Marzio [42] and Gibbs [19] approach (where S_c stands for the conformational entropy), we now have the entropy composed of two parts: $S = S_c + S_{th}$, where the thermal agitation part of the entropy, S_{th}, is included in the total entropy S.

7. The influence of anharmonic motion on the Hamiltonian

According to Kompaneyets [56], for the classical Hamiltonian we get

$$H_0 = -\frac{\hbar^2}{2m}\frac{d^2}{d\xi^2} + \frac{1}{2}m\omega^2\xi^2 \tag{23}$$

The fundamental energy levels E_n^0 are defined by use of wave-characteristic functions ψ_n^0 or ψ_n^{0*}

$$E_n^0 = \int \psi_n^{0*} H_0 \psi_n^0 d^3\xi \tag{24}$$

where ψ_n^0 stands for the characteristic wave function and ψ_n^{0*} for the complex-adjoined wave function; m represents the mass of the particle and $\hbar = h/2\pi$, where h is Planck's constant. For the case of a non-linear oscillator, the Hamiltonian H_o takes the form

$$H = \left(\frac{-\hbar^2}{2m}\frac{d^2}{d\xi^2} + \frac{1}{2}m\omega^2\xi^2\right) + A^*\xi^3 + B^*\xi^4 \tag{25}$$

or

$$H = H_0 + \vartheta \tag{26}$$

where

$$\vartheta = A^*\xi^3 + B^*\xi^4 \tag{27}$$

For the new energy levels E_n, we get

$$E_n = E_n^0 + \vartheta_{nm} \tag{28}$$

where

$$\vartheta_{nm} = \int \psi_n^{*0}\vartheta\psi_n^0 d^3\xi \tag{29}$$

The new energy levels for the anharmonic oscillator are shifted to new values of E_n. As a result of the anharmonic character of the motion, the partition function has to change to account for the different energy levels of the thermal energy motion [57] at T_g

$$\sum_{i=1}^{\infty} e^{-E_n^0/kT} \rightarrow \sum_{i=1}^{\infty} e^{-E_n/kT} \tag{30}$$

8. The phenomenon of hysteresis

For equilibrium conditions, the individual particles have to arrange themselves in a certain equilibrium distribution. Because the positions of individual particles ("sitting") are located at different energy levels, the following rules have to be satisfied

$$\frac{n_1}{n_0} = \frac{n_2}{n_1} = \frac{n_3}{n_2} \cdots \frac{n_{i+1}}{n_i} \tag{31}$$

where n_0 is the number of individual particles placed on the basic level, n_1 is the number of particles placed on the next level, etc. If for some reasons this rule is not satisfied, then we are dealing with an organized structure (non-equilibrium structure). Exactly this could happen in the vicinity of T_g, where the frequency jump of particles takes hours [47], while the "cooling–heating" cycle experiment takes minutes. Moreover, the partition function is characterized by a different set of energies below and above T_g. Therefore, for the particles it is almost impossible to achieve equilibrium distribution according to Eq. (31) (for a given temperature), and thus the system will be characterized by a smaller entropy. Such systems are called "organized structures". Any so-called "organized structure" will also show a small overshoot in the c_p values as the "organization" is removed. This means that the amorphous structure can display similar tendencies in the vicinity of T_g which are more pronounced for the crystalline structures at T_m. The physical reason for the irregularities in the amorphous system lies, however, in the deviations from equilibrium in the particle distributions. Deviations from equilibria can have a thermal (Eq. (31)) as well as a configurational character. The latter is usually well emphasized in the traditional approach [10, 11, 17–28]. Summarizing the results for two different shapes of the potential valleys [50, 51], we get

(a) $$U(\xi) = \frac{1}{2} f \xi^2 - \frac{1}{3} g \xi^3 \tag{32}$$

$$\alpha = \frac{1}{r_0} \frac{g}{f^2} k \tag{33}$$

$$\Delta\alpha = \frac{1}{r_0} \frac{g - g'}{f^2} k \tag{34}$$

$$c_p = k \left[1 + \frac{15}{g} \frac{g^2}{f^3} k T \right] \tag{35}$$

$$\Delta c_p = \frac{15}{9} \frac{(g^2 - g'^2)}{f^3} k T_g \tag{36}$$

In the more complex case where the term ξ^4 is included, the potential valley takes the form

$$\text{(b)} \qquad U(\xi) = \frac{1}{2} f \xi^2 - \frac{1}{3} g \xi^3 - \frac{c}{4} \xi^4 \tag{37}$$

The expressions for α and $\Delta\alpha$ do not change [51] and take the form of Eqs. (33) and (34). The term with ξ^3 represents the asymmetry of the mutual repulsion of atoms and the term with ξ^4 represents the softening of the vibrations at high amplitude. But the coefficient of c_p for the potential valley characterized by Ref. [36] will have a different expression [51]

$$c_p \approx k \left[1 + \left(\frac{3}{4} \frac{c}{f^2} + \frac{15 g^2}{9 f^3} \right) kT \right] \tag{38}$$

$$\Delta c_p \approx k T_g \left[\frac{3}{4} \frac{c}{f^2} + \frac{15 g^2}{9 f^3} \right] \tag{39}$$

provided that the functions c and g under T_g are much smaller than those above T_g. Looking back into general polymer physics [32–34], it is well established that (see also Eq. (2))

$$\Delta\alpha T_g = 0.113$$

If Eqs. (2) and (34) are comparable, this suggests that the product $(g - g')\, T_g$ must also be constant. (For the polymers, the bulk modulus at T_g can be considered as approximatively constant as well., Further experimental results [32, 34] such as those mentioned in Eqs. (3, 4)

$$\Delta c_p T_g \approx 25 \text{cal g}^{-1}$$

$$\alpha_1 T_g \approx 0.164$$

can be confirmed through Eqs. (34, 36) for $g' \to 0$. The function g represents the cohesive energy density and we can conclude that the higher the T_g temperature, the smaller the cohesive energy perturbation has to be to achieve the desired change into the liquid state.

9. The liquid at T_c and the origin of the p_c, V_c, T_c parameters

9.1. The critical temperature

The critical point phenomena can be studied from many different points of view [58–64] including the "scaling law", the multiple scales of length concept, or the theory of condensation [65]. For our investigation, we will apply the simple concept using the equations of state [8, 12–14, 66–72]. It can be noticed that many equations of state predict the easily visualized structure at T_c. So, for example, for the Dieterici equation [8] at T_c

$$V_c = 2b \tag{40}$$

In similar way, for van der Waals [8]

$$V_c = 3b \tag{41}$$

or for Peng–Robinson [66], (Fig. 11)

$$V_c = 3.9b \tag{42}$$

The model pictures of Eqs. (41)–(43) are shown on the Figs. 8–10. It can be seen from these figures that the critical state can be represented as a foam-like structure, in which the number of holes is practically disintegrating the liquid phase [8]. In the view of these pictures the overabundance of holes at T_c is the cause for the exclusion of the liquid phase. As will be shown later on, the T_c can also be related to the ratio of the cohesive energy and the energy of the thermal motion. As has been shown by Luck [73], the ratio of the density at $T=0$, ρ_O, to the density at $T=T^c$, ρ_c, can be expressed approximately by the logarithmic prime line dependence

$$\frac{\rho_o}{\rho_c} = 2 + \frac{2}{3}\log T_c \quad \text{for} \quad T_c > 1 \tag{43}$$

Thus for helium, the result $V_c = 2b$ fits the reality and for the majority of hydrocarbons the Peng–Robinson result is $V_c = 3.9b$.

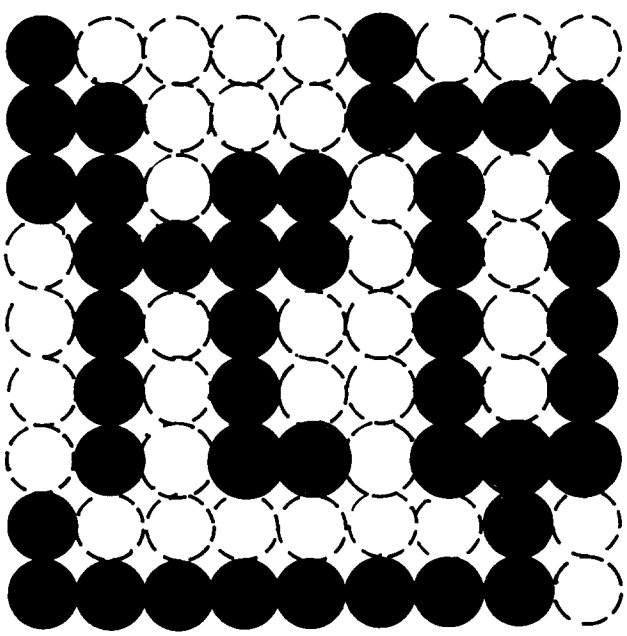

Fig. 8. The notion of a critical state in a two-dimensional model according to Hirschfelder et al. [8] explaining why, in the critical state, we have so many vacancies that the liquid phase loses continuity. According to this model, at the critical state we have about the same number of holes as particles. The total volume contains about 50% holes.

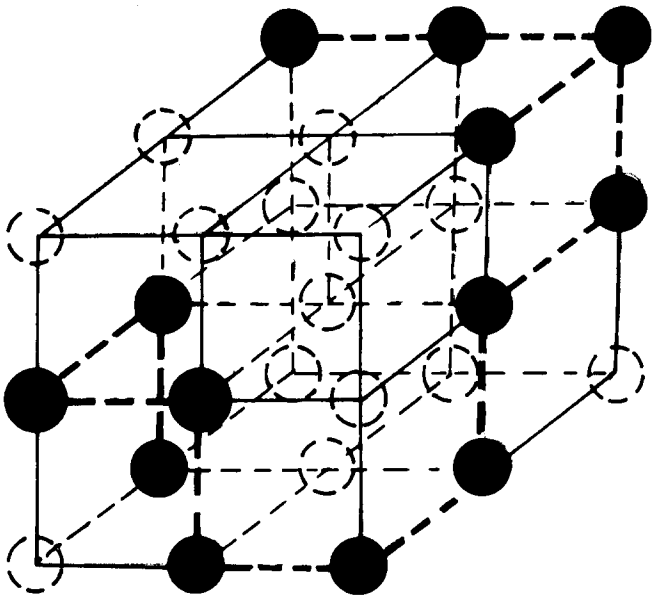

Fig. 9. The three-dimensional structure of $V_c = 2b$. The model is a convenient way to represent the critical state of helium, for which the ratio $V_c = 2b$ is roughly satisfied at T_c.

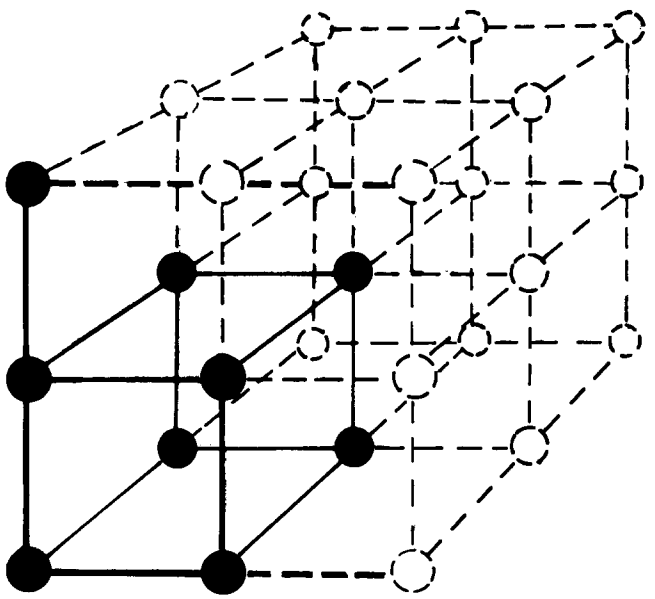

Fig. 10. The extrapolation of the two-dimensional case of Hirschfelder et al. [8]. Assuming that an increase in the number of holes will cause interruption of the phase in the vicinity of T_c, the number of holes will exceed the number of particles in the ratio of 1:2. In an area of typical p_c, 20–200 atm, the holes are assumed to be almost incompressible. (Note: $V_c = 3b$ for the van der Waals equation and hydrogen.)

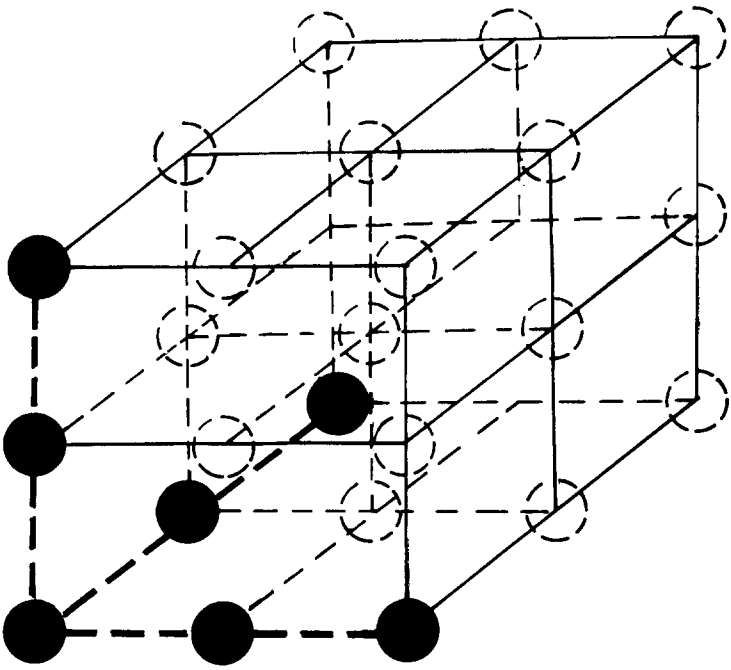

Fig. 11. The structure of the Peng–Robinson equation of state at $T = T_c$; $V_c = 3.9b$, valid for the vast majority of organic compounds.

9.2. *The critical pressure*

The meaning of the critical pressure was first elucidated by Hildebrand and Scott in connection with solubility parameter, δ, studies. For the solubility parameter δ, two different definitions exist [74]:

(a) The first is more general and is based on the evaporation energy L and on the molar volume V

$$\delta = \sqrt{\frac{L - RT}{V}} \tag{44}$$

(b) The second one assumes two types of coexisting interactions within the system or the system must be formed from two types of species, A and B. For the van der Waals parameters a and b, van Laar and Lorentz [75] and Hildebrand and Scott [76] have proposed

$$a = x_A^2 a_A + 2x_A x_B a_{AB} + x_B^2 a_B \tag{45}$$

$$b = x_A b_A + x_B b_B \tag{46}$$

and if for the mutual interaction a_{AB} geometrical averaging can take place

$$a_{AB} = (a_A a_B)^{1/2} \tag{47}$$

then the parameter δ can be expressed as

$$\delta = \frac{a^{1/2}}{b} \tag{48}$$

Because for the parameters a and b of the van der Waals equation [77]

$$a = \frac{27}{64}\frac{R^2 T_c^2}{p_c} \tag{49}$$

and

$$b = \frac{1}{8}\frac{RT_c}{p_c} \tag{50}$$

thus

$$\delta = \left(\frac{8}{27} p_c\right)^{1/2} \tag{51}$$

Please note that the van der Waals equation does not contain the temperature-dependent parameters a and b. To satisfy the experimental data for a few chosen solvents Hildebrand and Scott [74] had to modify the proportionality constant. For δ in cal cm^{-3} and p_c in atm, they obtained

$$\delta = 1.25\sqrt{p_c} \tag{52}$$

Eq. (52) predicts reasonably well the solubility parameters for n-hexane, diethylether, cyclohexane, CCl_4, benzene, CS_2, and $CHCl_3$ at 25°C. Through relation (52), the meaning of critical pressure can be understood.

For the δ parameter [78–80]

$$\delta^2 = \text{C.E.D.} \tag{53}$$

$$\delta^2 = \delta_d^2 + \delta_p^2 + \delta_h^2 \tag{54}$$

Connecting Eqs. (52), (53) and (54), we can say that the critical pressure is connected with the cohesive energy density C.E.D. and that the individual additions to the C.E.D. consist of individual contributions put together by dispersive (d), polar (p) and hydrogen (h) bond forces. The critical pressure also has a very high impact on the mutual solubility of the compounds. If two compounds have a similar δ parameter, such compounds (with few rare exceptions) are mutually soluble.

There seems, however, a certain arbitrariness in Hildebrand and Scott's approach:

(a) The factor of 1.25 was chosen empirically to agree with the experiment.
(b) δ was chosen for 25°C which does not have any relation to the individual T_c or T_g values for the individual components.

Therefore to develop the problem further, we propose the use of one of the most modern equations of state which can have a similar structure to Eqs. (48(–)51). Such an equation which can suite our means is the Peng–Robinson equation of state [66] which represents the triumph of modern thermodynamics. We will also compare the solubility parameters with the Peng–Robinson equation using Eq. (48) for one well-defined

temperature, namely the boiling point. Fig. 12 shows the T_B/T_C ratio for a few typical substances.

9.3. *The new approach to* p_c *interpretation*

According to Peng–Robinson [66], we get

$$\delta_{PR} = \frac{a^{1/2}}{b}$$

where

$$a(T) = a(T_C)\tilde{\alpha}(T_r, \omega)$$

$$b(T) = b(T_C) \tag{55}$$

$$\tilde{\alpha}^{1/2} = 1 + \kappa(1 - T_r^{1/2}) \tag{56}$$

$$\kappa = 0.37464 + 1.54226\omega - 0.26992\omega^2 \tag{57}$$

$$a(T_C) = 0.45724\frac{R^2 T_c^2}{p_c} \tag{58}$$

$$b(T_C) = 0.0778\frac{R T_c}{p_c} \tag{59}$$

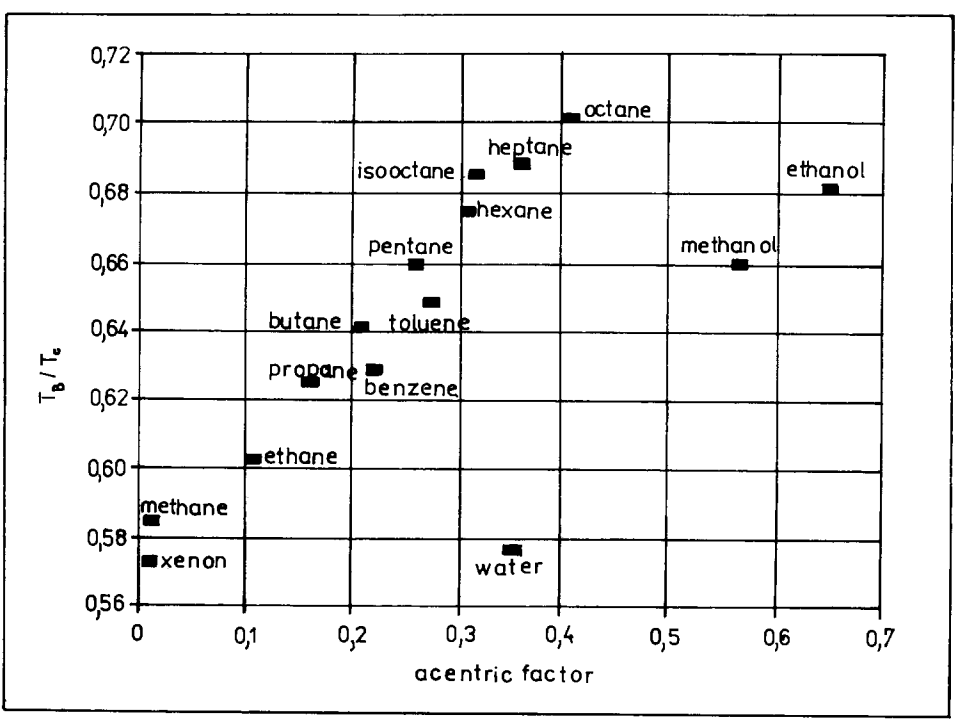

Fig. 12. The relative boiling point temperature as a function of Pitzer's acentric factor.

and

$$\delta_{PR} = \frac{\tilde{\alpha}^{1/2} a^{1/2}(T_c)}{b(T_c)} \tag{60}$$

for any particular temperature $T = T_B$

$$\delta_{BPR} = \tilde{\alpha}^{1/2}(T_{rB}) \frac{a^{1/2}(T_c)}{b(T_c)} \tag{61}$$

where δ_{PR} is the solubility parameter calculated according to Eqs. (55) and (60), where Eq. (55) was taken in analogy to Eq. (48); δ_{PR} is a temperature-dependent solubility parameter which also depends strongly on the Pizter acentric factor ω [13, 81, 82]. δ_{BPR} is δ_{PR} at the particular point $T = T_B$ and depends on T_B, $a(T_c)$, $b(T_c)$ and also strongly on Pitzer's acentric factor.

9.4. *The calculations and results*

Because the Peng–Robinson equation, together with Edmister's definition of the acentric factor [83], is able to connect the critical pressure with the cohesive energy density and the acentric factor only, we have used Eqs. (55)–(61) as the starting point for the proposed correlation below. The results based upon Eqs. (55)–(61), together with the experimental data and our correlations, are presented at the boiling point of the liquids in Table 1. It is possible to see that the Peng–Robinson equation, despite its perfect prediction of L, fails badly without modification to predict δ, defined through Eq. (55). This means either that the assumptions of Eqs. (45) and (47) based on the analogy of gravitational and electrical forces are probably generally not valid for the liquid state, or that the structure of the Peng–Robinson equation has to be modified for this purpose. However, the use of Eqs. (55)–(61) for the purpose of δ calculation can be achieved by very simple means.

As a first step, we search for the correction in the linear temperature shift in δ in the form of the linear temperature dependence in the vicinity of T_B. We assume

$$\delta_{COR,B} = \delta_{BPR} \frac{T_{rl}}{T_{rB}} \tag{62}$$

The shift in the temperature T_{rB} has a regular character for the individual substances (see also Fig. 12). The shift T_{rl} can be correlated as a straight line for only one parameter, ω (Fig. 13). This straight line has a general character for all substances, starting with the inert gases, paraffins or substances containing hydrogen bonds. This straight line can be defined as

$$T_{rL} = 0.501\,\omega + 0.395 \tag{63}$$

In Table 1 we can see the minimal deviation for the new approximation

$$\delta_{COR,B,1} = \delta_{BPR} \frac{T_{rl}}{T_{rB}} = \delta_{BPR} \frac{0.501\,\omega + 0.395}{T_{rB}} = \delta_{BPR} F_1(T_{rB}, \omega) \tag{64}$$

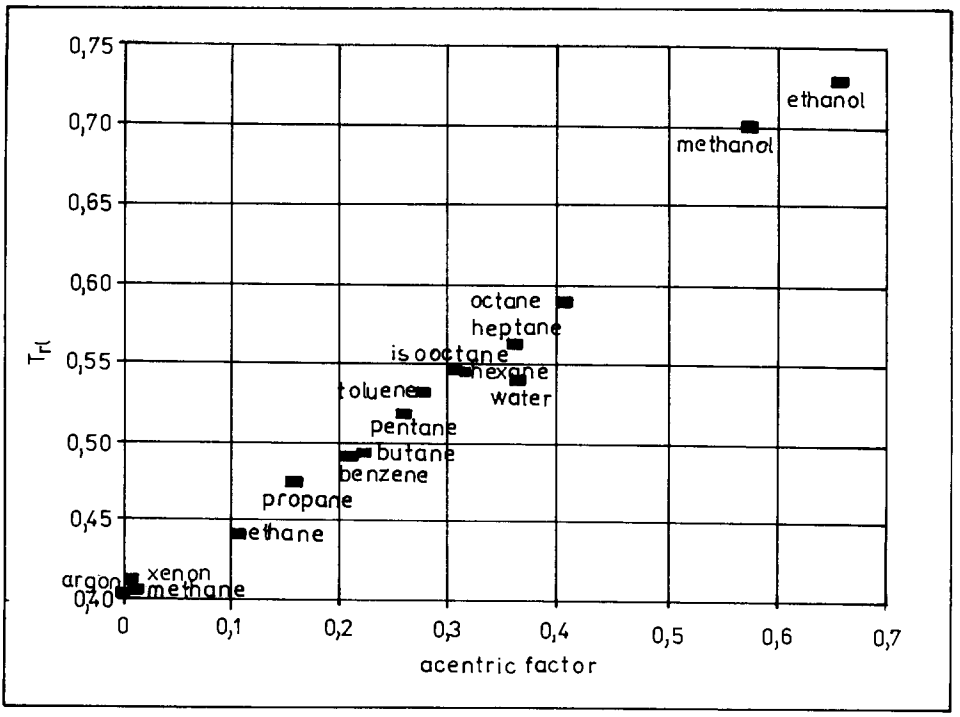

Fig. 13. The temperature of experimental data coincidence $T_{rl}/T_{rB} = \delta_{exp,B}/\delta_{BPR}$.

Also T_{rB} can be expressed for the different types of substances in dependence of ω. We get (see also Fig. 12)

$$T_{BR} = 0.314\omega + 0.577 \quad \text{for aliphatic alkanes}$$

$$T_{BR} = 0.350\omega + 0.553 \quad \text{for aromatics}$$

$$T_{BR} = 0.374\omega + 0.445 \quad \text{for substances containing the hydrogen bonds} \tag{65}$$

This way we can get from Eqs. (55)–(65)

$$\delta_{COR,B,2} = \delta_{BPR} F_2(\omega) = 8.6914\tilde{\alpha}^{1/2}(T_{rB})\sqrt{p_c}F_2(\omega) \tag{66}$$

From Table 1, we can see that the solubility parameter can be expressed within the minimal error interval through the square root of the critical pressure and the complex function of the acentric factor. The cohesive energy density is thus defined for low molecular weight substances through the critical pressure and its acentric factor. This seems to be valid quite generally. The function carrying the acentric factor influence $F_2(\omega)$, will be different for every type of substance essentially reflecting the fact that the boiling point T_{rB} is not a universal function of ω, while the T_{rL} temperature is. Note, please, that calculation of C.E.D. does not involve such values as T_c and V_c. An objection can be raised at this spot. By using Eqs. (65), six new empirical constants

Table 1
The values of δ for the experiment at the boiling point $\delta_{B,exp}$ and the individual correlations; $\delta \equiv [cal/cm^3]^{1/2}$. The deviations in % are taken relative to the experimental values

Substance	$\delta_{B,exp}$	δ_{BPR}	%	T_{rl}	T_{rL}	$\delta_{COR,B,1}$	%	$\delta_{COR,B,2}$	%
CH_4	6.8	9.79	−44	0.41	0.4	6.69	1.6	6.75	0.7
C_2H_6	7.6	10.34	−36.1	0.44	0.45	7.66	−0.8	7.58	0.3
C_3H_8	7.4	9.72	−31.4	0.48	0.47	7.36	0.5	7.34	0.8
C_4H_{10}	7.1	9.25	−30.3	0.49	0.5	7.17	−1	7.17	−1
C_5H_{12}	6.9	8.76	−27	0.52	0.52	6.94	−0.6	6.96	−0.9
C_6H_{14}	6.7	8.25	−24.8	0.55	0.55	6.67	0.4	6.7	0
C_7H_{16}	6.5	7.96	−22.5	0.56	0.57	6.61	−1.7	6.61	−1.7
C_8H_{18}	6.4	7.61	−18.9	0.59	0.59	6.45	−0.8	6.44	−0.6
CH_4O	15.4	14.48	6	0.7	0.68	14.83	6.7	14.94	3
C_2H_6O	13.8	12.88	6.7	0.73	0.72	13.54	1.9	13.46	2.5
H_2O	22.4	23.87	−6.6	0.54	0.57	23.75	6	23.66	−5.6
Benzene	8.3	10.57	−27.6	0.49	0.5	8.49	−2.3	8.49	−2.3
Toluene	8	9.75	−21.9	0.53	0.53	7.97	0.4	7.97	0.4
Argon	7	10.04	−43.4	0.41	0.39	6.81	2.7	–	–
Xenon	8	11.06	−38.3	0.41	0.4	7.7	3.8	–	–

characterizing the straight lines will enter into the calculations. This problem can be circumvented by using the Edmister definition of the acentric factor [83]

$$\omega = \frac{3}{7}\left\{\frac{\log p_c}{\frac{T_c}{T_B} - 1}\right\} - 1 \tag{67}$$

from which the ratio T_{rB}/T_c can be obtained

$$T_{rB} = \frac{1}{\frac{\log p_c}{\frac{7}{3}(\omega + 1)} + 1} \tag{68}$$

and substituted together with $\sqrt{T_{rB}}$ into Eqs. (56), (64) and (66).

By using Eqs. (56), (64), (67) and (68), the relation between δ and $\sqrt{p_c}$ and $F(\omega)$ can be obtained which will have a different form

$$\delta_{COR,B,3} = 8.6914\sqrt{p_c}F_3(\omega, \log p_c) \tag{69}$$

$\delta_{COR,B,3} \approx \delta_{COR,B,1}$ because the ω values obtained from the tabulated experimental data are almost identical to values of ω obtained based upon Eq. (67). Thus the T_{rB} calculated from Eq. (68) is distorted with minimal error (less than 1%). In this respect, p_c is determined mainly by the C.E.D. function which dominates in the perception of p_c and also is the complex form of Pitzer's acentric factor [13, 81, 82].

According to many authors, Pitzer's acentric factor is assumed to represent "the extra entropy change at evaporation" [74], or quoting Ref. [74]:

"Pitzer and his co-workers showed that these models are all consistent with an extended theory of corresponding states in which a third parameter expresses the effect of a finite core size regardless of the shape of the core. The third parameter, which they named "the acentric factor" was defined by the equation

$$\omega = -\log\left(\frac{p_s}{p_c}\right) - 1 \tag{70}$$

where p_s is the vapor pressure at reduced temperature 0.7."

We can see that the larger the ω, the lower the p_s. Therefore, ω can express the affinity of a substance for the liquid phase. With increasing molecular weight in parafins, for example, ω increases. Also for any polymer, ω has to be infinite because the polymer as the result of entanglements is unable to form the gas phase. $\omega \approx 0$ holds only for small spherical molecules such as CH_4 or He and Ar atoms. For a molecule which is held in the liquid phase by one centralized force to leave the liquid state is much more easy than for a molecule with a spacially dispersed bonding force. So the critical pressure (besides C.E.D.) also reflects the nature of the spacial bonding distribution by which the molecules are held in the liquid phase.

9.5. *The critical volume* V_c

The critical volume V_c seems to be clearly related to the electron polarizibilities of the individual atoms that form the system. This appears to be a very surprising statement, because the individual polarizibilities of atoms and molecules are certainly measured under completely different conditions [39, 46, 84, 85] than the p_c, V_c, T_c values and under these particular conditions are connected with the size of the atoms [38] forming the polarizibility ellipsoid for a given molecule. Table 2 shows the experimental values of the atomic polarizibilities of the individual elements in accordance with Le Fevre [86]:

$$P_c(\text{carbon}) = 1.0\ \text{Å}^3$$

$$P_H(\text{hydrogen}) = 0.4\ \text{Å}^3$$

$$P_o(\text{oxygen}) = 0.8\ \text{Å}^3$$

and adding 0.66 Å^3 for an isolated double bond and 0.533 Å^3 for a triple bond, we can see the connection between critical volume V_c and the individual polarizibilities of atoms. This means that the critical volume is defined by the high-frequency electronic orbitals of individual atoms.

The experimental value of the molecular polarizibilities quoted in column (2) of Tables 2–4 are taken from Ref. [87].

It seems to proper at this point to quote Verkoczy and Hlaváček [88]:

"From atomic polarizibilities [86] one can calculate the molecular polarizibilities fairly accurately [88]. However to obtain very accurate values for critical volume

Table 2
Table showing, for several compounds, the value of the critical volume in cm^3; the experimental electronic polarizibilities P_{exp} in $Å^3$; the polarizibilities based on the addition of polarizibilities of individual atoms $P_{mol} = \Sigma_{i=1}^{n} P_A$ in $Å^3$; and the ratio of $(V_c/N_{AV})\,(/P_c)$

Substance	V_c/cm^3	$P_{exp}/Å^3$	$P_{mol}/Å^3$	$V_c/N_{AV}\ 1/P_{exp}$
Ethane	148	4.47	4.4	55.1
Propane	200	6.29	6.2	52.8
Butane	255	8.12	8	52.1
Pentane	311	9.95	9.8	51.9
Hexane	368	11.78	11.6	51.86
Heptane	426	13.61	13.4	51.96
Octane	485	15.44	15.2	52.15
Nonane	543	17.35	17	51.96
Decane	602	19.1	18.8	52.53
Undecane	660	21.04	20.6	52.08
Dodecane	718	22.75	22.4	52.3
H_2O	45	1.45	1.6	51.5
Ethylene	124	4.26	3.6	48.33
Acethylene	113	3.33	2.8	56.33

Table 3
Table showing, for several aromatic hydrocarbons, the value of the critical volume V_c in cm^3; the experimental electronic polarizibilities P_{exp} in $Å^3$; the polarizibilities based on addition of the polarizibilities of individual atoms $P_{mol} = \Sigma_{i=1}^{n} P_A$ in $Å^3$; and the ratios $V_c/N_{AV}\ 1/P_{exp}$ and $V_c/N_{AV}\ 1/P_{mol}$

Substance	V_c/cm^3	$P_{exp}/Å^3$	$\frac{V_c}{N_{AV}}\frac{1}{P_{exp}}$	$P_{mol}/Å^3$	$\frac{V_c}{N_{AV}}\frac{1}{P_{mol}}$
Toluene	316	11.83	44.34	10.2	50.47
p-Xylene	378	13.7	45.8	12	52.29
Benzene	260	10.39	41.54	8.4	51.38
Naphthalene	408	17.48	38.68	13.2	51.3

calculations, the contribution for geometry, intermolecular interactions, lone electrons pairs, multiple bonds, the polarizibilities must be corrected for. For example for each secondary or tertiary branch, 0.06 $Å^3$ should be subtracted for each carbon atom. In the case of double bonds between carbon atoms, a value of 0.6 $Å^3$ should be added. Similarly a triple bond changes to 0.5 $Å^3$."

It should be remarked that the polarizibility is the tensor [38] and that even in the liquid phase aromatic molecules prefer "face-to-face" packing [38, 89] or the molecules can be made up from a few mutually penetrating ellipsoids. For aromatics, the polarizibility in the liquid phase can even be 40% lower than the polarizibility in the gas phase [89].

Comparing the values of $((V_c/N_{AV})\ (1/P_{mol}))$, we can see that even at the critical temperature the aromatics display a certain level of "face-to-face" packing. Exceptions

Table 4
Table analogous to the tables 2 and 3 for oxygen- or nitrogen-containing compounds (P_N (nitrogen) = 0.9 Å^3 [86])

Substance	V_c/cm^3	P_{exp}/Å^3	P_{mol}/Å^3	$\frac{V_c}{N_{AV}}\frac{1}{P_{exp}}$	$\frac{V_c}{N_{AV}}\frac{1}{P_{mol}}$
Furan	218	7.23	6.4	49.97	56.4
Ethanol	168.8	5.07	5.2	55.27	53.8
Propanol	220	6.77	7	53.95	52.1
Diethylamine	301	9.61	9.3	52	53.7
Triethylamine	394	13.38	12.9	48.8	50.6
Acetone	213	6.4	6.2	55.2	56.9
Methylethylketone	267	8.19	8	54.12	55.4
Diethylketone	336	9.93	9.8	56.1	56.8
Methylpropylketone	301	9.93	9.8	50.3	50.9
Acetic acid	171	5.15	5.2	55.12	54.6
Propionic acid	230	6.96	7	54.8	54.5
Butyric acid	290	8.58	8.8	56.1	54.6
Methylacetate	230	6.81	7	55.95	54.4

to this are: methanol with $((V_c/N_{AV})\ (1/P_{mol})) = 60.0$; methane with $((V_c/N_{AV})\ (1/P_{mol})) = 63.42$; and HCN and–CN groups with $((V_c/N_{AV})\ (1/P_{mol})) = 83.34$.

These substances show electron expansions or long-distance interactions (structural rebuilding) as a result of the temperature and pressure rise to p_c, V_c, T_c conditions. We can see that the size of the V_c volume is governed mainly by the polarizibilities of individual atoms and that the ratios of V_c relative to the summations of polarizibilities of individual atoms is quite regular. Therefore the size of V_c is decisively determined by fast vibrating electrons ($\omega_{el} = 10^{15}\ s^{-1}$). The frequency ω_{el} is the frequency with which the electron clouds shift their positions relative to the nucleus of the atoms.

10. Conclusions

In this paper, the liquid state is described as a foamy structure filled with holes and particles undergoing diffusional thermal motion. The holes function as inaccessible zones for the particles which are incompressible under low pressure values such as $p < p_c$. At T_g, only very few holes appear (2.5%) and their number grows linearly above T_g. Also at T_g, the character of the thermal motion starts to change (from harmonic to anharmonic), which itself can lead to a sudden increase in the coefficient of thermal expansion α, as well as to a stepwise increase in c_p values. This was emphasized and presented quantitatively in this paper. Above T_g however, as Brownian motion starts to develop, the configurational approach (which is traditional in the literature) starts to play a bigger role. At T_c, the number of holes grow rapidly (almost exponentially) and by taking them as inaccessible zones, the disintegration of the liquid phase occurs in

such a way that the impossibility of a liquid phase existing above T_c can be visualized using models representing the most common equations of state. From the Peng–Robinson equation of state (using the Edmister definition of the acentric factor), the critical pressure of liquids seems to be connected to the cohesive energy density and to the acentric factor only. A first approximation for the critical volume of a vast majority of substances can be obtained from the polarizibilities of individual atoms through their summation. Multiplying this value by a factor of 50–55, we can get the size of V_c. We also have to correlate the size of V_c for the presence of isolated double bonds, triple bonds, etc. The critical volume seems to be connected additively to the electronic structure of individual atoms which form the compound.

References

[1] M. Reiner, Rheology, in S. Flügge (Ed.), Handbuch der Physik, Springer-Verlag, Berlin Göttingen, Heidelberg, 1958, p. 36.
[2] A.J. Batschinski, Z. Phys. Chem., 84 (1913) 643.
[3] G. Tamman, Aggregatzustände, Leipzig, 1922.
[4] G. Tamman, Der Glaszustand, Leipzig, 1933.
[5] J.H. Hildebrand, Viscosity and Diffusivity, J. Wiley & Sons, New York, London, 1977, p. 15, p. 99.
[6] R.B. Bird, W.E. Stewart and E.N. Lightfoot, Transport Phenomena, J. Wiley & Sons, New York, 1965, p. 39.
[7] W.W. Graesley, Viscoelasticity and flow in polymer melts and concentrated solutions, in J.E. Mark (Ed.), Physical Properties of Polymers, Am. Chem. Soc., Washington D.C., 1984, p. 97.
[8] J.O. Hirchfelder, C.F. Curtiss and R.B. Bird, Molecular Theory of Gases and Liquids, J. Wiley & Sons, New York, 1954, p. 250, p. 284, p. 311.
[9] J. Frenkel, Kinetic Theory of Liquids, Dover Publications Inc., New York, 1955, p. 93, p. 140.
[10] F. Bueche, Physical Properties of Polymers, J. Wiley & Sons, New York, London, 1954, p. 106, p. 202.
[11] J.D. Ferry, Viscoelastic Properties of Polymers, J. Wiley & Sons, New York, London, 1961, p. 267, p. 352.
[12] J.J. Martin, Ind. Eng. Chem. Fund., 18 (1979) 2.
[13] K.S. Pitzer, D.Z. Lippman, R.F. Curl, CH.M. Huggins and D.E. Petersen, J. Am. Chem. Soc., 77 (1955) 3133.
[14] L. Riedel, Z. Electrochem., 4 (1949) 222.
[15] A.L. Lyndersen, Report No. 3, College of Engineering, The University of Wisconsin, Madison, Wisconsin, 1965.
[16] D.H. Kaelble, Free volume and polymer rheology, in F.R. Eirich (Ed.), Rheology, Vol. 5, Academic Press, New York, London, 1969, p. 223.
[17] A. Eisenberg, The Glassy State and Glass Transition, in J.E. Mark (Ed.), Physical Properties of Polymers, Am. Chem. Soc., Washington D.C., 1984, p. 55.
[18] M. Gordon, Thermal properties of high polymers, in P.D. Ritchie (Ed.), Physics of Plastics, London ILIFFE Books Ltd., Princeton, New Jersey, D. Van Nostrand Company Inc., 1965, p. 208.
[19] J.H. Gibbs, J. Chem. Phys., 25 (1956) 185.
[20] V.G. Rostishavili, V.I. Irirzshak and B.A. Rosenberg, Steklovanie polymerov, Chimija, Leningrad, 1987.
[21] I. Havlíček, V. Vojta, M. Ilavský and J. Hrouz, Macromolecules, 13 (1980) 357.
[22] I. Havlíček, M. Ilavský and J. Hrouz, J. Macromol. Sci. Phys., B21, 3 (1982) 425.
[23] A. Kovacs, Relaxation Phenomena in Polymers, Longworth (Ed.), Interscience, 1974.
[24] A. Kovacs, J. Polym. Sci., 30 (1964) 131.
[25] J. Šesták, Thermochim. Acta, 95 (1985) 459.
[26] J. Šesták, J. Therm. Anal., 33 (1988) 75.

[27] J. Jackle, Philos. Mag., 44 (1981) 533.
[28] J. Šesták, Wiss Zeitschr. Friedrik-Schiller Univ. Jena: Math. Natur., 32 (1983) 377.
[29] P.J. Flory, Proc. R. Soc., London, A234 (1956) 60 & 73.
[30] M.L. Williams, J. Phys. Chem., 59 (1955) 95.
[31] M.L. Williams, R.F. Landel and J.D. Ferry, J. Am. Chem. Soc., 77 (1955) 3701.
[32] R. Simha and R.F. Boyer, J. Chem. Phys., 37 (1962) 1003.
[33] R.F. Boyer and R. Simha, J. Polymer. Sci., B33 (1973) 11.
[34] R.F. Boyer, J. Macromol. Sci., B7 (1973) 487.
[35] S.C. Sharma, L. Mandelkern and F.C. Stehling, Polym. Lett., 10 (1972) 345.
[36] G. Adam and J.H. Gibbs, J. Chem. Phys., 43 (1965) 139.
[37] R.A. Hayes, J. Appl. Polym. Sci., 5 (1961) 318.
[38] H. Mark and A.V. Tobolsky, Physical Chemistry of High Polymeric Systems, Interscience Publishers, New York, 1940, p. 37, p. 105, p. 119.
[39] J.A. Brydson, Plastics Materials, Butterworths, England, 4th edn., 1982, p. 75, p. 109, p. 203.
[40] R. Becker, Z. Phys. Chem., Leipzig, 258 (1977) 953.
[41] R. Becker, Plaste Kautch., 25 (1978) 1.
[42] U.T. Kreibich and H. Batzer, Angew. Makromol. Chem., 83 (1979) 57.
[43] B. Hlaváček, V. Khunová and M. Večeřa, Collect. Czech. Chem. Commun., in press.
[44] Z. Chvoj, J. Šesták and A. Tříska, Kinetic Phase Diagrams; Non-Equilibrium Phase Transitions, Elsevier, Amsterdam, 1991.
[45] E.A. Di Marzio, J.H. Gibbs, P.D. Fleming III and I.C. Sanchez, Macromolecules, 9 (5) (1976) 736.
[46] B. Meissner, V. Zilvar, The Physics of Polymers, SNTL-Praque, 1987, p. 94, 260.
[47] W. Kauzman, Chem. Rev., 43 (1948) 219.
[48] B. Wunderlich, J. Phys. Chem., 64 (1960) 1052.
[49] Technical Trade Literature, British Resin Products Ltd., London, 1980.
[50] Ch. Kittel, W.P. Knight and M.A. Rudermann, Berkley Physics Course, Mechanics, Vol. 1., New York, McGraw-Hill, 1965, p. 227–229.
[51] Ch. Kittel, Introduction to Solid State Physics, J. Wiley & Sons, New York, 3rd edn., 1966, p. 184, 195.
[52] F.H. Müller, Thermodynamic of deformation, in F.R. Eirich (Ed.), Rheology, Vol. 5, Wiley & Sons, New York, London, 1969, p. 417.
[53] J.C. Slater, Introduction to Chemical Physics, Dover Publications Inc., New York, 1939, p. 222.
[54] F.T. Wall, Chemical Thermodynamics, W.H. Freeman and Company, San Francisco, 1958, p. 287.
[55] W.A.P. Luck, How to understand liquids, in P.L. Huyskens (Ed.), Intermolecular Forces, Springer-Verlag, Berlin, Heidelberg, New York, 1991, p. 55.
[56] A.S. Kompaneyets, Theoretical Physics, Dover Publications Inc., New York, 1962, p. 89, 265.
[57] R.W. Gurney, Introduction to Statistical Mechanics, Dover Publications Inc., New York, 1966, p. 39.
[58] K.G. Wilson, The Renormalization Group and Critical Phenomena, The Nobel Lecture, December 8th., 1982.
[59] M.E. Fisher, The Theory of Equilibrium Critical Phenomena, Rep. Progr. Phys., 30 (1967) 615.
[60] K.G. Wilson, Sci. Am., 241 (1979) 158.
[61] M.E. Fisher, J. Phys. Soc. Jpn., 26 (1969) 87.
[62] M.E. Fisher, J. Math. Phys., 5 (1964) 944.
[63] L.E. Kadanoff, Physics, 2 (1966) 263.
[64] L.E. Kadanoff, Rev. Mod. Phys., 39(2) (1967) 395.
[65] M.E. Fisher, Physics, 3 (1967) 255.
[66] D.Y. Peng and D.B. Robinson, Ind. Eng. Chem. Fund., 59 (1976) 15.
[67] O. Redlich and J.N.S. Kwong, Chem. Rev., 44 (1949) 233.
[68] M. Benedict, G.B. Webb and L.C. Rubin, J. Chem. Phys., 8 (1940) 334.
[69] M.A.J. Michels and H. Meijer, Fluid Phase Equilibria, 11 (1983) 19.
[70] M.M. Abbott, Cubic equations of state, in K.C. Chao and R.L. Robinson (Eds.), Equations of State, Eng. and Research, Adv. in Chemistry Series, 182 (1979) 47.
[71] B.I. Lee and W.C. Edmister, Ind. Eng. Chem. Fund., 10, 1 (1971) 33.
[72] G. Soave, Chem. Eng. Sci., 27 (1972) 1197.
[73] W.A.P. Luck, Angew, Chem., 91 (1979) 408.

[74] J.H. Hildebrand and R.L. Scott, The Solubility of Nonelectrolytes, Reinhold Pub. Corp., New York, 3th edn., 1958, p. 425, 430.
[75] Y.J. Van Laar and Z. Lorentz, Anorg. Chem., 146 (1925) 42.
[76] J.H. Hildebrand, J.M. Prausnitz and R.L. Scott, Regular and Related Solutions, Van Nostrand Reinhold Company, New York, 1970, p. 82, p. 89.
[77] J.CH. Forman and G. Thodos, A.I.Ch.E J., 4, (1958) 356.
[78] C.M. Hansen, Ind. Eng. Chem. Prod. Dev., 8 (1969) 2.
[79] P.A.J. Small, J. Appl. Chem., 3 (1953) 71.
[80] H. Burrell, Interchem. Rev., 14 (1955) 3.
[81] K.S. Pitzer and G.O. Hultgren, J. Am. Chem. Sci., 80 (1958) 4793.
[82] K.S. Pitzer, J. Am. Chem. Soc., 77 (1955) 3427.
[83] W.C. Edmister, Petroleum Refiner, 37 (1958) 4.
[84] W. Holzmüller and K. Altenburg, Physik der Kunststoffe, Akademie-Verlag, Berlin, 1961, p. 480.
[85] W.J. Moore, Physical Chemistry, Prentice Hall Inc., Englewood Cliffs, New Jersey, U.S.A. 4th edn., 1972, p. 698.
[86] R.J.W. Le Fevre, Adv. Phys. Organ. Chem., 3 (1965) 1.
[87] K.Y. Kang and M.S. Jkon, Theor. Chim. Acta Berlin, 61 (1982) 41.
[88] B. Verkoczy and B. Hlaváček, The Structure of Liquids and the Equation of State, Saskoil-Internal Report, Req. Saskatchewan, 1985.
[89] M.I. Schachparonow, N.M. Nedbajev and M.S. Tunin, Zh. Fiz. Chim., 58 (11) (1983) 2746.